Int. J. Multiphase Flow Vol. 9, No. 6, pp. 649–663, 1983
Printed in Great Britain.

0301-9322/83 $3.00 + .00
Pergamon/Elsevier

A SCATTERING LIGHT PROBE FOR THE MEASUREMENT OF OCEANIC AIR BUBBLE SIZES

F. AVELLAN
Institut de Mécanique Statistique de la Turbulence, Laboratoire Associé au C.N.R.S., Université d'Aix-Marseille II, 13003 Marseille, France et Laboratoire de la Mécanique des Fluides, Ecole Polytechnique Fédérale de Lausanne, 1015 Lausanne, Suisse

and

F. RESCH
Institut de Mécanique Statistique de la Turbulence, Laboratoire Associé au C.N.R.S., Université d'Aix-Marseille II, 13003 Marseille, France et Université de Toulon, U.E.R. Sciences et Techniques, La Garde, France

(*Received* 28 *September* 1981; *in revised form* 13 *December* 1982)

Abstract—A new optical probe has been designed, tested, calibrated and used in a bubbly two-phase flow. The probe is based on the principle of light scattering at an angle of ninety degrees from an incident laser beam. The errors inherent in such a technique are reviewed and evaluated. The calibration curve shows that the output voltage is proportional to the square of the bubble diameter. A first test is presented in a real bubbly flow produced by the action of wave-breaking in an air–sea interaction simulating facility.

1. INTRODUCTION

Measurement of two-phase flow characteristics is of a great importance in many fields of fundamental and engineering sciences.

For example, the production of marine aerosols by bubble bursting at the sea surface is of special interest for oceanographers and environment specialists. Such studies have been carried out for the last twenty years by, for example, Blanchard & Woodcock (1957, 1980), Blanchard (1963) and McIntyre (1972). Unfortunately, the bubble size distribution due to wave-breaking in seawater is still unknown with sufficient precision (Resch 1982). The main reason for lack of data is due to the fact that there are no measurement techniques available adapted to this particular application. It is, indeed, necessary to be able to detect bubble size in a range of approx. 50 μm–5 mm, see Resch & Avellan (1978).

Several techniques are used to measure the bubble size distribution of an air–water two-phase flow, see Jones & Delhaye (1976). For example, fiberglass optical probes have been developed by Danel & Delhaye (1971). Conical hot-film probes have been used by Resch *et al.* (1974) to determine the two-phase flow characteristics within the bubbly turbulent part of the hydraulic jump. Unfortunately, the extreme range of values of bubble sizes mentioned above does not allow the use of such material probes. In order to choose an appropriate method, a careful review of the different techniques such as acoustical, chemical, mechanical, electrical and optical, was made. These techniques are listed in table 1 with their characteristics, their advantages and disadvantages. Among others, Medwin (1977), Keller (1972) are to be cited for their attempt at using acoustical and optical methods respectively, in the above-mentioned range of bubbles. In the present study a local optical probe has been selected and a prototype has been designed and made. It has been tested and calibrated under specific conditions. The errors inherent in its principle have been carefully analyzed and evaluated. Finally, the probe has been used to detect the air bubbles entrained in water by the action of wave-breaking. Experiments have been carried

Table 1. Review of various techniques for bubble (or droplet) detection

	TECHNIQUES	PHASE DETECTED	SIZE RANGE	SOURCE OF ERRORS	DATA TREATMENT	COMMENTS
GLOBAL TECHNIQUES	Chemical method	Water	-.-	Chemical constants	Simple	Use as a reference method
	Impaction method	Air	Micronic	Evaporation	Long and tedious	Perturbation of flow by the impigers
	Electronic precipitation	Air	10^{-3} μm- 1μm	Collectors	Automatic	Perturbation of the flow
	Acoustical attenuation	Water	30μm- 600μm	Bubble acoustics	Automatic FFT method	Promising method
	Light scattering	Air Water	1μm- 500μm	Numerical resolution and energy distribution	Numerical treatment complex and difficult	Delicate for unknown distributions
	Light attenuation	Air Water	10μm- 10^{3} μm	Noise of photomultiplier	Automatic, fast	Simple technique
LOCAL TECHNIQUES	Light scattering at small angles	Air Water	.1μm- 10μm	Noise of photomultiplier	Automatic, complex	For narrow range
	Light scattering at an angle of ninety degrees	Air Water	Bubbles: 50μm-5mm Drops: .2 μm-500μm	Noise of photomultiplier, definition of the sensing volume	Automatic, fast	Calibration of the probe

out in the large air–sea interaction simulating facility at the Institut de Mécanique Statistique de la Turbulence (I.M.S.T.), Aix-Marseille II University.

2. SCATTERING LIGHT PROBE

2.1 *Choice of the techniques and principle of operation*

The scattering light method was chosen because it essentially makes possible the local measurement of the particle size which is convenient in external flow. Another reason for the choice of light scattering was the fact that many instruments using the same technique were developed for aerosol sizing in the atmosphere. The basic principle of this kind of instrument is that the light flux scattered by a spherically-shaped particle present in a volume of detection is a direct function of its diameter, see van der Hulst (1957), and for the applications of the method Ederhof (1976), Holve & Self (1979). The operating principle is schematically represented in figure 1, where the ninety degrees collection case is illustrated. The illuminating system includes a laser beam associated with a diaphragm and optical lenses. The detection system is composed of a lens, a diaphragm and a photomultiplier. The sensing volume can be determined by the intersection of a cylinder, the axis of which is the same as the axis of the collecting lens, with the incident beam defined by the light intensity distribution—usually Gaussian with an HeNe laser—as an elliptic cylinder.

On the one hand, if the size distribution of an aerosol with different particles involving different relative refractive indexes had to be calculated, it would be necessary to overcome the sensitivity of the instrument to the variation in the indexes. Hence, it is necessary to choose a light-collected direction close to the forward scattering direction (Holve & Self 1979). However, in this case the sensing volume should have slot ends and a non-uniform light distribution along a transverse section of the sensing volume. Consequently, we would be obliged to take this into account by inversion techniques as did Holve and Self. On the other hand, if a particular scatter is of interest, such as bubbles in seawater, one should have selective response of the instrument leading to a collecting lens direction of 90°. Furthermore, in this case, the light intensity is uniformly distributed in a cross-section of the straight cylindrical sensing volume if its diameter is smaller than the laser beam width.

In the range of bubble diameters considered, i.e. 50 μm–5 mm, optics allows several levels of approximations to predict the light intensity scattered in one direction. Davis' calculations (1955) are based on refraction and reflection laws and show that, for angles near to the 90° direction (82.8°–100°), only the first reflected rays have to be accounted for. Kingsbury & Marston (1981) using both physical optics approximations and

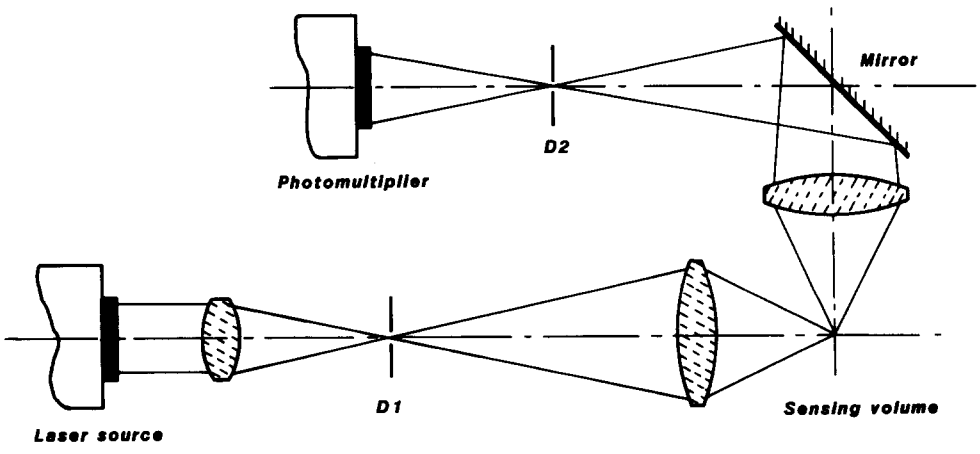

Figure 1. Principle of operation of the scattering light probe.

Mie-scattering algorithms found near the critical angle ($\sim 82.8°$) coarse and fine structures due to interference effects.

By using a large aperture to filter fine structures and by collecting the light in a region where no coarse oscillations appear, i.e. for angles greater than the critical angle, these interference effects can be overcome and the Davis approximation remains valid.

In our work the receiving optics of the probe was set up with an angular aperture of 14° leading to collection angles between 83 and 97° which correspond to the conditions mentioned above.

In these circumstances most of the light collected is obtained from that first reflected on the bubble surface. The collected flux ϕ can thus be determined, see Avellan (1980), by integrating the intensity I of the light reflected over the solid angle Ω bounded by the angular aperture U of the receiving optical system, figure 2

$$\phi = \int_{\Omega} I \, d\Omega \qquad [1]$$

If I_0 is the intensity of the incident beam supposed to be collimated and uniform, we can write, according to Davis

$$I = (1 - \eta) \frac{d^2}{16 f^2} I_0 \qquad [2]$$

where d is the bubble diameter, f the focal length of the receiving optical system and η the part of the light intensity lost by refraction. The coefficient η is given by Fresnel's formulas and it depends only on the relative refractive index of air in water and the incident light angle.

In this way, the flux collected is given by

$$\phi = \frac{I_0}{4\pi f^2} \int_{\Omega} (1 - \eta) \, d\Omega \cdot \frac{\pi d^2}{4}. \qquad [3]$$

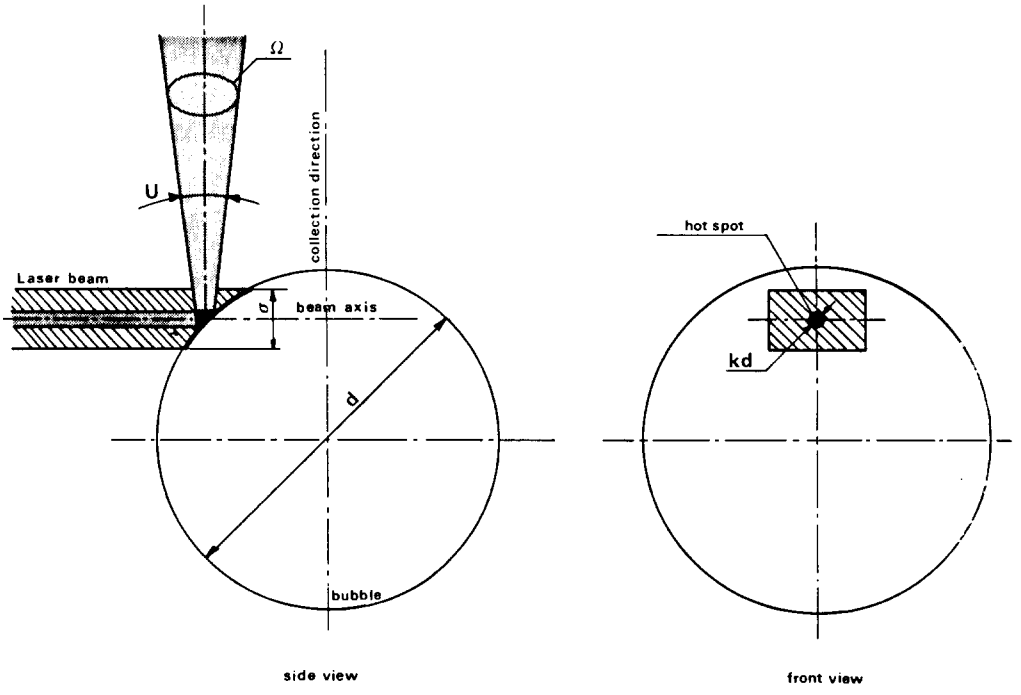

Figure 2. Reflection of the laser beam on the bubble surface.

This shows that the flux is directly proportional to the cross-section of the bubble because the integral in [3] is independent of the bubble size. Furthermore, only that part of the bubble surface subtended by the solid angle Ω participates in the light flux effectively collected by the receiving optical system. By using reflection laws and setting the condition that the light reflected should fall in the receiving lens, we can determine this part as the "hot spot" of figure 2.

The characteristic dimension $k \cdot d$ of such a spot which is close to the circular form in the case of small apertures can be determined, Avellan (1980), leading to the following expression for k:

$$k = \left(\frac{1 - \cos U/2}{2}\right)^{1/2}.$$

For an angle of 14° the value of k is 6.1×10^{-2}.

Although a uniform light intensity is assumed in [2], the laser distribution is in fact Gaussian. To be consistent with [2], the spot diameter kd should then be limited in such a way that the light intensity varies by a few per cent within the hot spot. For instance, if a maximum variation of 1% only is allowed, this yields a maximum spot diameter kd_m of

$$kd_m = 0.28\sigma, \quad \text{i.e. } d_m \simeq 5\sigma$$

where σ is the laser beam width.

However, provided that the range of the bubble diameters is below the upper limit d_m, [3] shows a simple relation between the bubble diameter and the flux collected, allowing the use, after calibration, of such a probe in various bubbly two-phase flow configurations.

2.2 *Description of the probe*

Starting with the schematic diagram of figure 1, a prototype of the probe was designed and built by a French company (A.I.D., Grenoble, France), see figure 3.

The light source is made from a 2 mW He–Ne laser tube ($\lambda = 0.6328\ \mu$m). As the transverse distribution of the light intensity is Gaussian, only the central part of the beam is utilized in order to obtain a uniform distribution within the sensing area. This is achieved by means of a cylindrical lens associated with a 300 μm wide slit. A transmitting objective is made of two lenses. The scattered light is reflected by a mirror towards the photomultiplier through a diaphragm with a diameter of 500 μm. Thus the sensing volume is approximately well represented by a cylinder with a 500 μm dia. and a height of 300 μm as shown in figure 4. An interferential filter has been added ahead of the photomultiplier to shield the probe from the influence of ambient light.

The photomultiplier (P.M.) is selected to detect very small light fluxes. It is directly coupled with a current voltage converter. All these components are assembled in a waterproof stainless steel case, see figure 3.

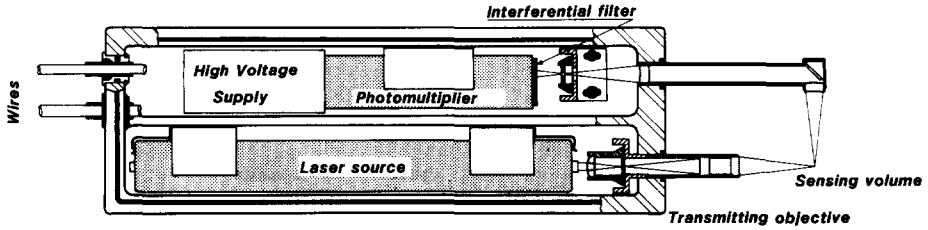

Figure 3. Cross-section of the optical probe prototype.

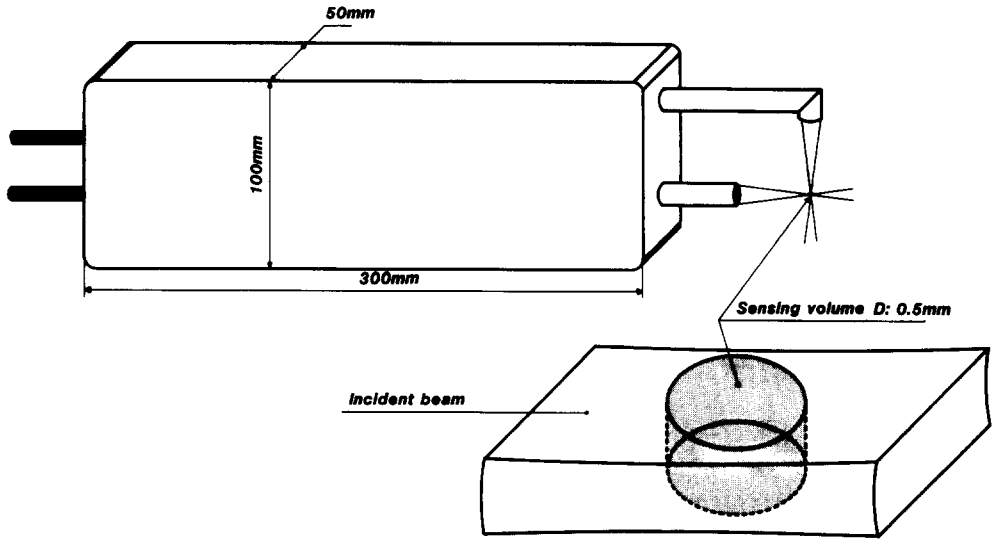

Figure 4. The optical probe and its sensing volume.

3. ANALYSIS OF THE OUTPUT SIGNAL

In order to obtain a correct statistical estimate of the granulometry it is necessary to investigate carefully the possible sources of error affecting the signal and the data processing. Two kinds of errors should be considered, one related to the physical processes involved, the other to the statistical methods used.

3.1 *Errors due to physics*

These kinds of difficulties are mainly caused by the finite dimensions of the sensing volume which can be considered, in a first approximation, as a cylinder of diameter D and volume v (as will be seen in the following paragraph). They arise when two bubbles are present at the same time in the detection volume or when a bubble partially crosses this same volume.

Coincidence effects. Coincidence effects arise from the fact that there is a non-zero probability of having more than one bubble at the same time in the sensing volume. If n is the mean concentration of particles per unit volume, then the average number n of particles present in the sensing volume v is:

$$n = n \cdot v.$$

If the particles are supposed to be randomly distributed in the flow, then the probability of observing N particles at the same time in the volume v is given by Poisson's law

$$P(N) = \frac{n^N e^{-n}}{N!}.$$

Therefore the geometrical dimensions of the sensing volume should be chosen in such a way that n is less than 1. If this condition is fulfilled, the error due to the coincidence effects is less than:

$$\frac{P(2)}{P(1)} = \frac{n}{2}.$$

Side effects. The output signal may be biased by the relative positions of the bubble crossing the sensing volume as shown in figure 4.

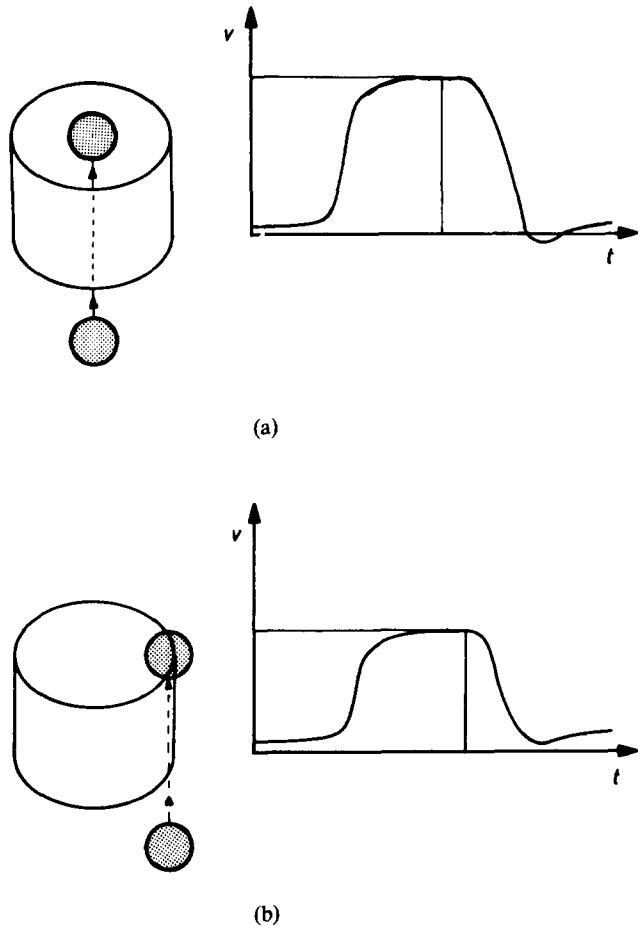

Figure 5. Typical output signal when a bubble crosses the sensing volume, (a) the bubble is completely detected; (b) the bubble is only partially detected.

The shape of the output signal is determined by the three periods of the crossing (figure 5):—the bubble penetrates the volume—the bubble is entirely present in the volume—the bubble is leaving the volume. The maximum amplitude of the signal is then proportional to the square of the diameter d. If the same bubble is only partially crossing the sensing volume the shape of the signal will be the same, but the maximum amplitude will be reduced as in figure 5. The bubble will therefore be detected as a smaller bubble leading to the so-called "side-effect error".

To take this effect into account, [3] should be modified as follows:

$$V = K \cdot I_0 \psi(d, \rho) \frac{\pi}{4} (dk)^2 \qquad [4]$$

where $V = K\phi$, K is the total sensitivity of the system in Volt/Candela and V the output voltage. ψ is a function of the bubble diameter d and the distance ρ between the axis of the sensing volume and the bubble centre, as schematically represented in figure 6.

The function ψ will have the following values:

$\psi = 1$ if the bubble is fully detected (figure 4a)
$\psi < 1$ if the bubble is partially detected (figure 4b)
$\psi = 0$ if the bubble is not detected.

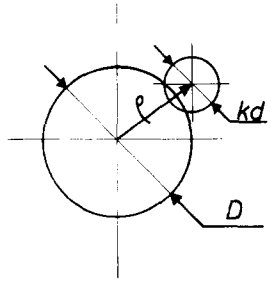

Figure 6. Schematic of the relative position of a bubble of apparent diameter kd and the sensing volume of diameter D.

If we assume that the image of the bubble is circular with an apparent diameter kd the above values are obtained as follows, see figure 5:

$$\psi(d, \rho) = 1 \quad \text{when} \quad 0 < \rho < \frac{D - kd}{2}$$

$$0 < \psi(d, \rho) < 1 \quad \text{when} \quad \frac{D - kd}{2} < \rho < \frac{D + kd}{2}$$

$$\psi(d, \rho) = 0 \quad \text{when} \quad \rho > \frac{D + kd}{2}.$$

In our case, I_0 is independent of ρ as explained in the paragraph following [3], thus [2] may be written in a more concise form:

$$V = \alpha\psi(d, \rho)d^2 \qquad [5]$$

where V is now a function of d and ρ. Hence, the system (V, d, ρ) is considered as a system of three random variables governed by [5]. Using statistical tools we show that the following relation can be obtained (see Avellan 1980).

$$f(d) = \frac{(D + kd)^2}{(D - kd)^2}\left\{2\alpha d g(\alpha d^2) + \int_d^{+\infty} \frac{16 d X' X(kd, d^2/y^2)}{y^2(D + ky)^2} f(y)\, dy\right\}. \qquad [6]$$

where g is the probability density of the signal reduced to its maximum amplitude and f is the size distribution.

The function $X(kd, t)$ is the reciprocal function of the function ψ.

Therefore:

$$X(kd, t) = \frac{D - kd}{2} \quad \text{when} \quad t = 1$$

$$\frac{D - kd}{2} < X(kd, t) < \frac{D + kd}{2} \quad \text{when} \quad 0 < t < 1$$

$$X(kd, t) = \frac{D + kd}{2} \quad \text{when} \quad t = 0.$$

$X'(kd, t)$ is the derivative of $X(kd, t)$ with respect to t. The relation (6) is a Volterra integral equation which can be solved for the function f, if the function X (and X') can be determined. The integral equation takes into account the "side effect". If k tends to zero it is reduced to a relation between f and g with the side effect neglected:

$$f_0(d) = 2\alpha d g(\alpha d^2) \qquad [7]$$

From [6] it is possible to have an estimate of the "side effect error" Δ_0/f_0 giving an upper value as follows:

$$\frac{\Delta f_0}{f_0} = \frac{4\epsilon}{(1-\epsilon)^2} \qquad \text{with} \qquad \epsilon = \frac{kd}{D} \qquad [8]$$

We can check that this error is small for small bubble diameters (at the limit $f_0(0) = f(0)$) and increases with the apparent diameter kd as shown in figure 7, leading to a value of 110% corresponding to the maximum diameter d_m for which [4] remains valid.

3.2 *Errors due to statistics*

Let us consider the estimate $g(v)$ of the probability density of the signal. The mean square error $(\Delta g/g)^2$ for a window Δv smaller than 20% of the standard deviation, see Bendat and Piersol (1971), is:

$$\left(\frac{\Delta g}{g}\right)^2 = \frac{1}{N \Delta v g(v)} \qquad [9]$$

where N is the number of particles detected; N is an increasing function of the volume v and of the total duration of the measurement.

This error will be small if N is large, i.e. if the sensing volume is large and/or the duration of the experiment is long and/or the concentration is large.

It may be seen that the sensing volume should be optimized by increasing its diameter

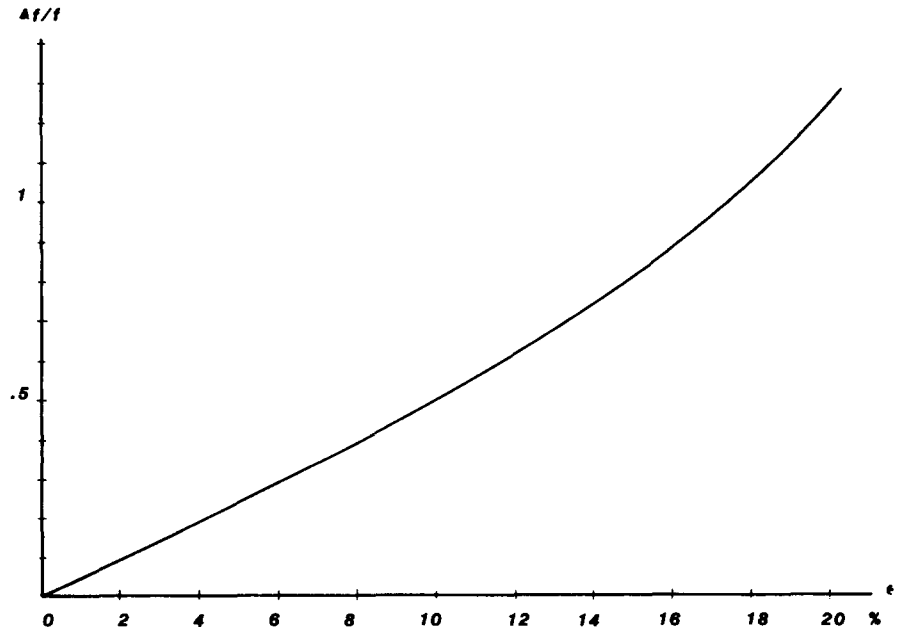

Figure 7. Estimate of the maximum error due to the side effect.

to reduce side effects and statistical errors and by reducing its diameter to overcome coincidence possibility. The balance between coincidence and side effect errors depends on the concentration. However, statistical errors can be decreased by increasing the measurement time.

4. EXPERIMENTAL STUDIES

4.1 *Data acquisition*

In order to obtain good statistical stability it is necessary to increase the data acquisition time. Furthermore, the sampling rate should be high enough to have a signal resolution which permits the detection of the maximum peak of each signal burst associated with a bubble. The two constraints lead to conditional sampling techniques to overcome the problem of storing a tremendous amount of data. A hardware technique is used, see sketch in figure 8, based on a logic gate triggered by each bubble passage to the sensing volume.

4.2 *Calibration of the probe*

As previously indicated, the probe has to be calibrated to be used in real flows. Bubbles of known diameters are produced by means of glass capillary tubes. This generation technique has been described in detail by Blanchard (1963). Paying special attention to cleanliness, it is possible to produce bubbles with a given diameter for a sufficient period of time.

A calibration unit was specially built, see the schematic diagram in figure 9. The

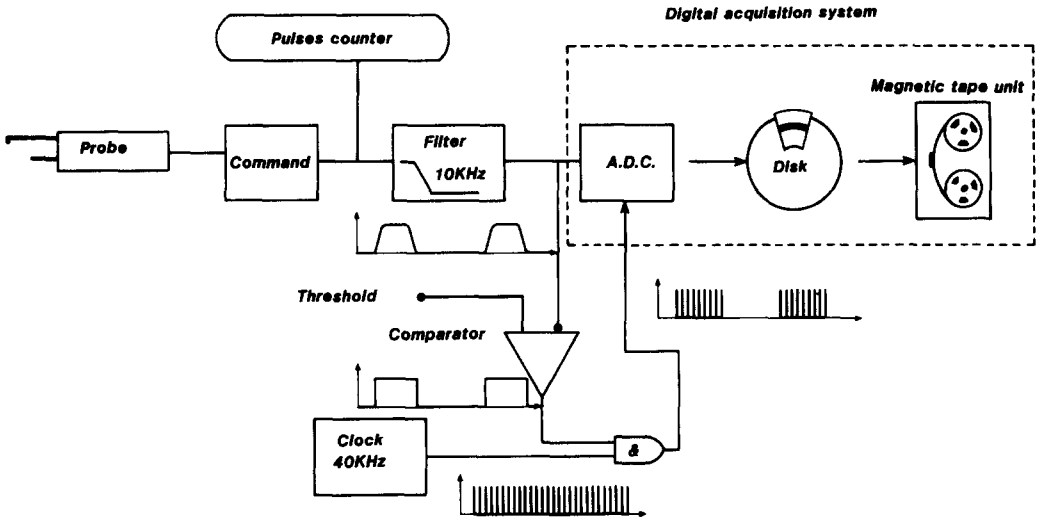

Figure 8. Flow chart of the data acquisition system.

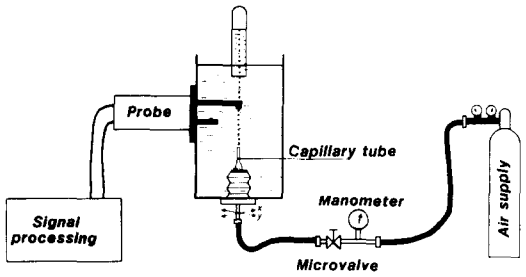

Figure 9. Calibration system of the probe.

capillary tube is oriented in such a way that all the bubbles produced move up through the sensing volume of the probe and are completely detected. They are then collected in a calibrated tube. An electronic counter gives the number of bubbles sensed: this allows us to determine the bubble diameter with a rather good and reproducible precision (applying corrections for air compressibility). For each bubble diameter, around 5000 bubbles were detected giving one calibration point (voltage vs diameter). Using various capillary tubes we obtain the calibration curve giving the sensitivity coefficient α of the probe. In figure 10 are reported voltage histograms of selected points (figures 10a and 10b) and in figure 11 the calibration curve. The histograms such as those shown in figures 10(a) and 10(b) may be subject to discussion as they should have been narrower. It is possible that some changes in the bubble diameter occurred during the calibration recording. In all cases the maximum value has been selected as shown by the small arrow. As expected the voltage output is proportional to the square of the bubble diameter.

4.3 *Use of the probe in a bubbly flow produced by breaking waves*

Breaking waves were generated in the large air–sea interactions simulating facility of I.M.S.T. (see Coantic *et al.* 1969 for a description) with a wind blowing at 14 m/s and with

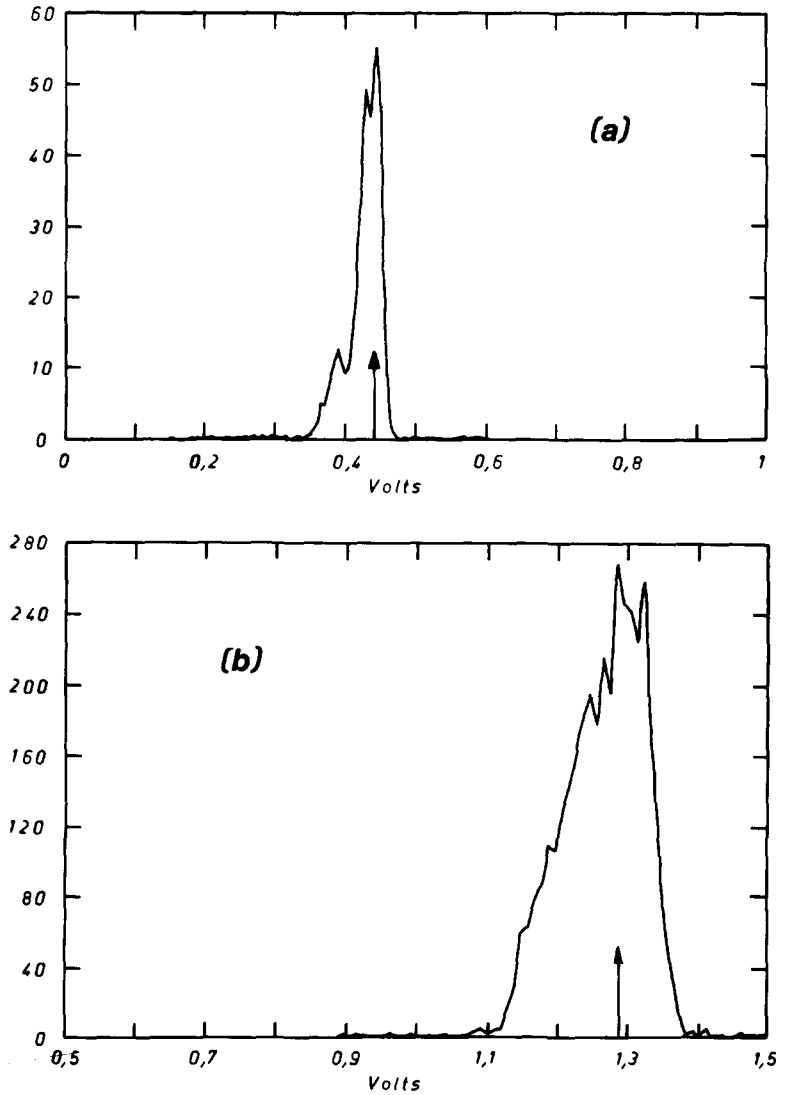

Figure 10. Typical voltage histograms obtained during probe calibrations.

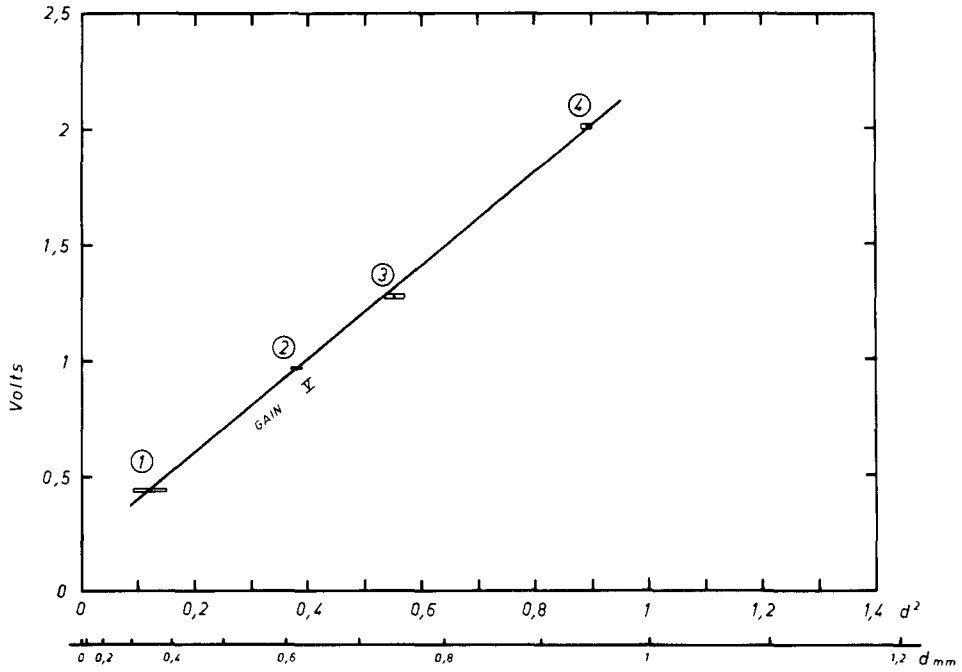

Figure 11. Probe calibration curve.

the additional use of the mechanical wave-maker. The breaking action produces a large number of bubbles of various shapes in the water. The position of the probe is shown in figure 12. The time recording was about 3 hr leading to a total number of 517 bubbles detected. The normalized voltage histogram is shown in figure 13. Normalization scales are the number of bubbles (517) and the window width ($\Delta V = 126$ mV). A certain number (29) of bubbles larger than 2 mm were found (corresponding to 8 V), but were not evaluated, as the gain of the photomultiplier was purposely limited. An estimate of the bubble size distribution is shown in figure 14 using [7], i.e. neglecting the side effect error. The confidence intervals were evaluated using [9] and display a wide scatter in the data due to the rather small number of bubbles detected.

5. CONCLUSION

An optical probe based on light scattering at an angle of ninety degrees from the incident light beam was selected, designed, tested and calibrated for measurement of

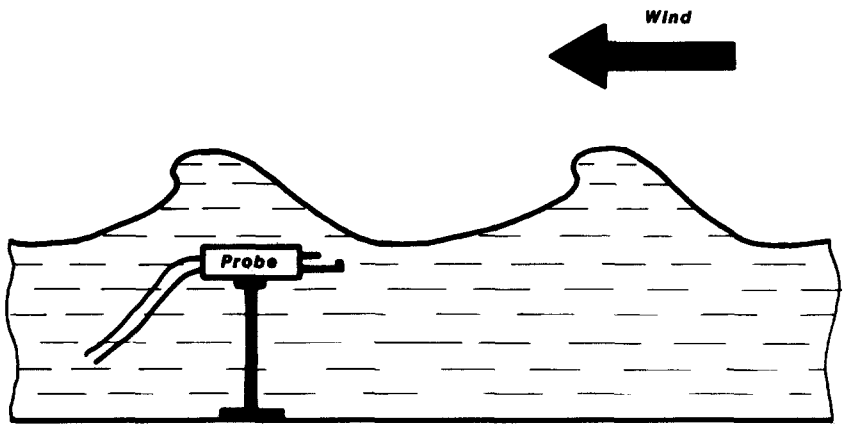

Figure 12. Experimental set-up for breaking wave experiments.

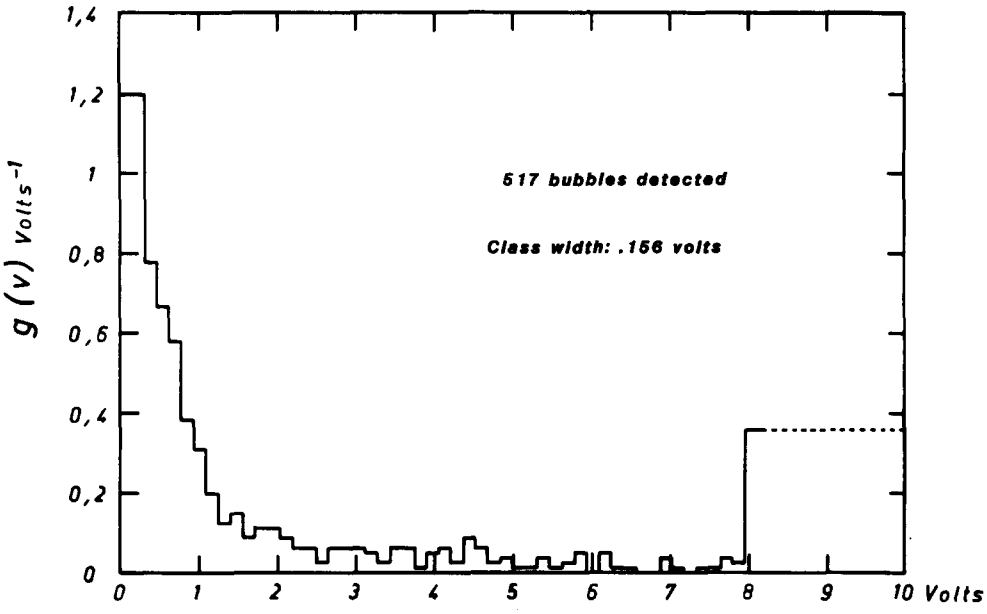

Figure 13. Normalized histogram of voltages observed under breaking waves.

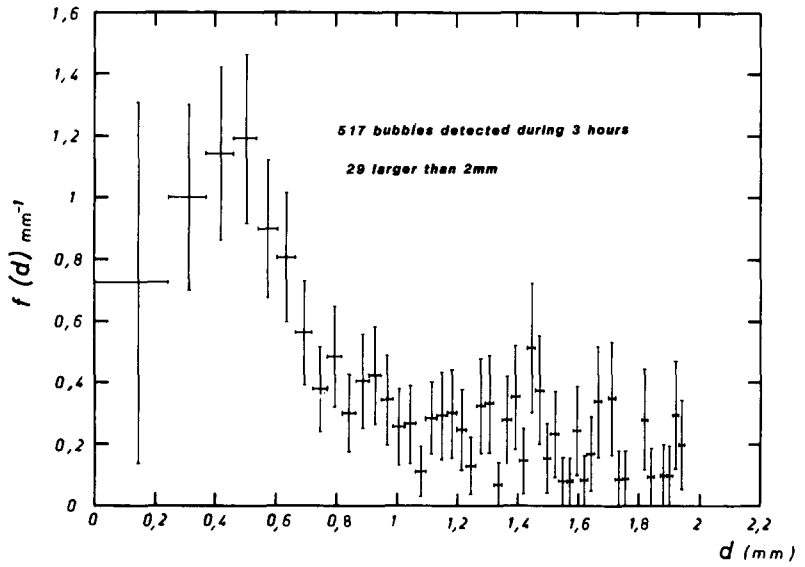

Figure 14. Bubble spectra under breaking waves.

bubble diameters in the range 200 μm–2 mm. This range could easily be extended to 50 μm–5 mm by increasing the sensing volume and the photomultiplier sensitivity.

The various possible errors which may affect such a probe are carefully reviewed. An estimate of the maximum error is given when feasible.

The prototype of the probe is described as well as the data acquisition and processing system used. The probe is calibrated with a specially designed unit. The calibration curve is, as expected, a straight line, if output voltage is plotted vs the square of the bubble diameter.

Finally the result of a first test is displayed showing the size distribution of a population of bubbles produced by breaking waves. Although the first result is widely scattered it shows clearly that such a probe can be used with success in such conditions. We should

mention that the lack of data in that particular area is now crucial; geochemists, specialists in air–sea particle exchanges and aerosol production need to know such size spectra. For the first time a local optical probe using light scattering at ninety degrees for *in situ* bubble-size measurement has been developed and used successfully. Geometrical arrangements have to be made to adapt the various parameters governing the physical processes, i.e. different concentrations and sizes with depth in water.

Acknowledgements—The authors wish to acknowledge the contribution of individuals and organizations which made this research possible. They specially thank all their colleagues from I.M.S.T. and in particular M. Coantic and A. Ramanonjiarisoa as well as members of the technical staff including M. Bourguel, P. Chambaud and B. Zucchini. They also wish to thank F. Danel of A.I.D. for his valuable contribution in designing the prototype of the probe. This research was made possible by financial support from the "Centre national de la recherche scientifique" and the "Centre national pour l'exploitation des océans" (Grant No. 80/2196).

REFERENCES

AVELLAN, F. 1980 Caractéristiques diphasiques des échanges particulaires à l'interface air-mer: étude météorologique. Thèse de Docteur-Ingénieur, I.M.S.T., Université d'Aix-Marseille, France.

BENDAT, J. S. & PIERSOL, A. G. 1971 *Random Data: Analysis and Measurements Procedures*. Wiley–Interscience, New York.

BLANCHARD, D. C. 1963 The electrification of the atmosphere by particle from bubbles in the sea. *Prog. Oceanography* **1**, 73–202.

BLANCHARD, D. C. & WOODCOCK, A. H. 1957 Bubble formation and modification in the sea and its meteorological significance. *Tellus* **9**, 145–158.

BLANCHARD, D. C. & WOODCOCK, A. H. 1980 The production, concentration and vertical distribution of the sea-salt aerosol. *Ann. N.Y. Acad. Sci.* **338**, 330–347.

BOURGUEL, M., RESCH, F. & COANTIC, M. 1979 Description d'un système numérique d'acquisition et de prétraitement des données. Rapport I.M.S.T., Marseille, France.

COANTIC, M., BONMARIN, P., POUCHAIN, B. & FAVRE, A. 1969 Etude d'une soufflerie pour recherches sur les échanges d'énergie atmosphère océan. AGARD. C.P. no. 48.

DANEL F. & DELHAYE, J. M. 1971 Sonde optique pour mesure de taux de présence local en écoulement diphasique. *Mesure, Régulation, Automatisme no août-septembre*, 99–101.

DAVIS, G. E. 1955 Scattering of light by an air bubble in water. *J. Opt. Soc. Am.* **45**, 572–581.

HOLVE, D. & SELF, S. A. 1979 Optical particle sizing for *in situ* measurements. *Appl. Opt.* **18**, 1632–1652.

KINGSBURY, D. L. & MARSTON, P. L. 1981 The scattering near the critical angle of bubbles in water. *J. Opt. Soc. Am.* **71**, 358–361.

EDERHOF, A. 1976 A light-scattering probe for droplets size and wetness fraction measurement in two-phase flows. *Two-Phase Steam Flow in Turbines and Separators* (Edited by MOORE, M. J. & SLEVERDING, C. H.). Hemisphere, London, pp. 249–260.

JONES, O. C. & DELHAYE, J. M. 1976 Transient and statistical measurement techniques for two-phase flows: a critical review. *Int. J. Multiphase Flow* **3**, 89–116.

KELLER, A. 1972 The influence of the cavitation nucleus spectrum on cavitation inception, investigated with a scattered light counting method. *J. Basic Engng* **94**, 917–925.

MCINTYRE, F. 1972 Flow patterns in breaking bubbles. *J. Geophys. Res.* **77**, 5211–5228.

MEDWIN, H. 1977 In situ acoustic measurements of microbubbles at sea. *J. Geophys. Res.* **82**, 971–976.

RESCH, F. J. 1982 Air sea particulate exchanges in coastal regions. Reprinted from Preprint Volume: First International Conference on Meteorology and Air–Sea Interaction of the Coastal Zone, 10–14 May, 1982: The Hague, Netherlands. Published by the American Meteorological Society, Boston, Mass.

RESCH, F. J., LEUTHEUSSER, H. J. & ALEMU, S. 1974 Bubbly two-phase flow in hydraulic jumps. *J. Hydraulics Div., A.S.G.E.* **100**, No. HY1, Proc. Paper 10297, 137–149.

RESCH, F. & AVELLAN, F. 1978 Aspects diphasiques des échanges particulaires à l'interface air-mer. Etude d'une instrumentation. *La Houille Blanche* **5**, 337–340.

VAN DER HULST, H. C. 1957 *Light Scattering by Small Particles*, pp. 114–130. Wiley, New York.